

MULTISTATIC PASSIVE DETECTION OF CYCLOSTATIONARY SIGNALS

*S. Horstmann*¹, *D. Ramírez*^{2,3}, and *P. J. Schreier*¹

¹ Signal and System Theory Group, University of Paderborn, Germany

² Dept. of Signal Theory and Communications, Universidad Carlos III de Madrid, Spain

³ Gregorio Marañón Health Research Institute, Madrid, Spain

ABSTRACT

In this work we consider a multistatic passive detection problem, which is motivated by a multiple-input multiple-output (MIMO) passive radar application. Specifically, we consider a single illuminator of opportunity (IO) and several surveillance and reference arrays for the detection of a Gaussian cyclostationary signal in temporally colored and spatially correlated noise. Concretely, 1) we derive the generalized likelihood ratio test (GLRT) for this problem and 2) provide a stochastic representation of the test statistic under the null hypothesis, which allows us to set the threshold for a constant probability of false alarm. Monte Carlo simulations are carried out to investigate the performance of the proposed GLRT.

Index Terms— Cyclostationarity, generalized likelihood ratio test (GLRT), multistatic passive radar.

1. INTRODUCTION

This paper considers a multiple-input multiple-output (MIMO) passive multistatic radar system, which consists of one transmitter and multiple multichannel receivers. The goal is to detect the presence of a cyclostationary target echo at multiple surveillance arrays given the measurements at the surveillance and reference arrays. Many techniques have been derived to approach this problem based on different assumptions. The most common and intuitive approach for single-input single-output (SISO) signal detection is based on cross-correlating the signals at surveillance channel (SC) and reference channel (RC) [1–6]. Although this resembles the matched filter, it is suboptimal due to noise at the RC [6]. Further bistatic setups are considered in [7–9], where generalized likelihood ratio tests (GLRTs) were derived for the case of unknown stochastic waveforms and for various assumptions on the signal and noise models for MIMO channels. In our previous works [10–12], we derived the GLRTs for different noise assumptions and an LMPIT-inspired test for the

bistatic passive detection of cyclostationary signals, which we also refer to as two-channel detection problem since there is only a single SC and a single RC. The GLRTs for the case of unknown deterministic waveforms and different assumptions on signal and noise models were presented in [13, 14]. Bayesian tests were derived in [13, 15].

The authors in [14] derived the GLRT for the multistatic detection problem, i.e., for multiple reference and surveillance arrays, considering unknown deterministic waveforms. Moreover, the authors discussed the benefits of centralized processing approaches and compared it to similar detectors encountered in active MIMO radar and passive source localization problems. In [16], the authors proposed an ad-hoc detector based on the generalized coherence [17]. A GLRT for a passive MIMO radar is proposed in [18] for unknown channel coefficients and colored Gaussian noise provided there is secondary training data available.

In this work we consider the multistatic passive radar problem and derive the GLRT for the detection of a Gaussian cyclostationary signal in temporally colored and spatially correlated noise given multiple surveillance and reference arrays. In order to ensure a constant false alarm rate, we also provide a stochastic representation of the test statistic under the null hypothesis that allows for determining the threshold. It is shown that the distribution under the null is given by a product of independent random beta variables. The performance of the proposed GLRT is compared to the state-of-the-art by means of numerical simulations.

2. PROBLEM FORMULATION

Let us consider a scenario with J surveillance antenna arrays and K reference antenna arrays. We assume that all arrays are equipped with L antennas, although the results could be generalized to different numbers of antennas at each array. The single IO is assumed to be equipped with L_I antennas. A noisy version of its transmission signal is received at the reference arrays. In the presence of a reflecting target, there will also be a noisy version of the IO signal present at the surveillance arrays whereas there is only noise if no target echo is present.

The work of D. Ramírez was partially supported by MCIN/AEI/10.13039/501100011033/FEDER, UE, under grant PID2021-123182OB-I00 (EPiCENTER) and by the Office of Naval Research (ONR) Global under contract N62909-23-1-2002.

Assuming that the target echo is synchronized in Doppler-shift and time-delay with the direct-path signal propagating from IO to the reference array, the problem can be formulated as follows:

$$\begin{aligned} \mathcal{H}_0 : \quad & \mathbf{u}_{s,j}[n] = \mathbf{v}_{s,j}[n], \quad j = 1, \dots, J, \\ \mathcal{H}_1 : \quad & \mathbf{u}_{s,j}[n] = \mathbf{H}_{s,j}[n] * \mathbf{s}[n] + \mathbf{v}_{s,j}[n], \quad j = 1, \dots, J, \end{aligned} \quad (1)$$

and reference signals under both hypotheses: $\mathbf{u}_{r,k}[n] = \mathbf{H}_{r,k}[n] * \mathbf{s}[n] + \mathbf{v}_{r,k}[n]$, $k = 1, \dots, K$. Furthermore, $\mathbf{H}_{s,j}[n] \in \mathbb{C}^{L \times L_I}$ and $\mathbf{H}_{r,k}[n] \in \mathbb{C}^{L \times L_I}$ represent the time-invariant frequency-selective channels from the IO to the surveillance and reference arrays, respectively. The additive independent noise terms $\mathbf{v}_{s,j}[n] \in \mathbb{C}^L$, $j = 1, \dots, J$, and $\mathbf{v}_{r,k}[n] \in \mathbb{C}^L$, $k = 1, \dots, K$, are assumed to be wide-sense stationary (WSS) with arbitrary temporal and spatial correlation.

The IO signal $\mathbf{s}[n] \in \mathbb{C}^{L_I}$ is discrete-time zero-mean second-order CS with cycle period P . For this reason $\mathbf{u}_{r,k}[n] = \mathbf{H}_{r,k}[n] * \mathbf{s}[n] + \mathbf{v}_{r,k}[n]$ is also CS with cycle period P and so are, under the alternative, $\mathbf{u}_{s,j}[n] = \mathbf{H}_{s,j}[n] * \mathbf{s}[n] + \mathbf{v}_{s,j}[n]$. Hence, the goal is to detect cyclostationarity at the surveillance arrays. Moreover, we assume that $L_I \geq L$, which implies that the cyclic (cross) power spectral densities (PSD) of $\mathbf{H}_{s,j}[n] * \mathbf{s}[n]$ and $\mathbf{H}_{r,k}[n] * \mathbf{s}[n]$ have full rank L .

The model above assumes that there is no clutter, interference, or direct-path signal present at the RC and SC. This may be achieved by either physical shielding [19] or cancellation through signal processing techniques presented in e.g. [3, 20]. Admittedly, the complete cancellation of direct-path interference in the SC is an idealized assumption as pointed out in [20]. A more sophisticated model considering the direct-path interference is approached in [6, 21, 22] but they do not exploit cyclostationarity. The time-delay of the target echo is inherently accounted for in the frequency-selective channels in our model. Moreover, considering that direct-path interference has zero Doppler-shift as opposed to the target path signal, it can be filtered [23].

3. DERIVATION OF THE GLRT

In order to detect the presence of cyclostationarity at the SCs, we exploit the results from [24], where the GLRT for the detection of cyclostationarity in a single channel has been derived. Assuming Gaussianity, the problem boils down to a test for the structure of the covariance matrix. Specifically, the covariance matrix of a vector-valued WSS signal $\mathbf{u}_{s,j}[n]$, $j = 1, \dots, J$, is Hermitian block-Toeplitz with block size L . Under the alternative, $\mathbf{u}_{s,j}[n]$, $j = 1, \dots, J$, is cyclostationary with cycle period P and the covariance matrix is again Hermitian block-Toeplitz but with block size LP . Additionally, the cross-covariance matrices of $\mathbf{u}_{s,i}[n]$ and $\mathbf{u}_{s,j}[n]$ are non-zero and block-Toeplitz with block size LP .

The authors in [24] show that the maximum likelihood estimate of a block-Toeplitz structured covariance matrix of a Gaussian distribution can be approximated by a block-circulant matrix, which allows for a closed-form solution. Based on these results, we first stack NP observations of $\mathbf{u}_{s,j}[n]$ and $\mathbf{u}_{r,k}[n]$ into two vectors $\mathbf{w}_{s,j} \in \mathbb{C}^{LNP}$ and $\mathbf{w}_{r,k} \in \mathbb{C}^{LNP}$, respectively. Noting that a block-circulant matrix can be block-diagonalized by the DFT matrix, we transform the observations into the frequency domain:

$$\begin{aligned} \mathbf{z}_{s,j} &= (\mathbf{L}_{NP,N} \otimes \mathbf{I}_L)(\mathbf{F}_{NP} \otimes \mathbf{I}_L)^H \mathbf{w}_{s,j}, \\ \mathbf{z}_{r,k} &= (\mathbf{L}_{NP,N} \otimes \mathbf{I}_L)(\mathbf{F}_{NP} \otimes \mathbf{I}_L)^H \mathbf{w}_{r,k}, \end{aligned}$$

where \mathbf{F}_{NP} is the DFT matrix of dimension NP , $\mathbf{L}_{NP,N}$ is the commutation matrix, and the matrix $(\mathbf{L}_{NP,N} \otimes \mathbf{I}_L)$ permutes the observations such that $\mathbf{z}_{s,j}$ and $\mathbf{z}_{r,k}$ contain N blocks of P frequencies, which are separated by multiples of the cycle frequency $2\pi/P$. When the signals are cyclostationary, these frequencies are correlated. Hence, under the null hypothesis the covariance matrices of $\mathbf{z}_{s,j}$ are block-diagonal with block size L , whereas the cross covariance matrices of $\mathbf{z}_{s,i}$ and $\mathbf{z}_{s,j}$ for $i \neq j$ are zero. Under the alternative, the (cross) covariance matrices of $\mathbf{z}_{s,i}$ and $\mathbf{z}_{s,j}$ are block-diagonal with block size LP and so are the (cross) covariance matrices of $\mathbf{z}_{r,k}$ and $\mathbf{z}_{r,l}$, for $k, l = 1, \dots, K$.

Now, we can put the pieces together to establish the structure of the covariance matrix of \mathbf{z} under both hypotheses, where $\mathbf{z} = [\mathbf{z}_s^T \ \mathbf{z}_r^T]^T \in \mathbb{C}^{(J+K)LNP}$ with $\mathbf{z}_s = [\mathbf{z}_{s,1}^T \ \dots \ \mathbf{z}_{s,J}^T]^T \in \mathbb{C}^{JLNP}$ and $\mathbf{z}_r = [\mathbf{z}_{r,1}^T \ \dots \ \mathbf{z}_{r,K}^T]^T \in \mathbb{C}^{KLNP}$. Under the null hypothesis we obtain

$$\mathbf{S}_0 = \mathbb{E}[\mathbf{z}\mathbf{z}^H | \mathcal{H}_0] = \begin{bmatrix} \mathbf{S}_s^{(0)} & \mathbf{0} \\ \mathbf{0} & \mathbf{S}_r \end{bmatrix},$$

where the off-diagonal blocks are zero since observations at SC and RC are uncorrelated. Here, $\mathbf{S}_s^{(0)} = \mathbb{E}[\mathbf{z}_s \mathbf{z}_s^H | \mathcal{H}_0]$ is a block-diagonal Hermitian matrix with block size L and $\mathbf{S}_r = \mathbb{E}[\mathbf{z}_r \mathbf{z}_r^H]$ is a $K \times K$ Hermitian block matrix, where each block of dimension $LNP \times LNP$ is a block-diagonal matrix with block size LP . Now, under \mathcal{H}_1 , the covariance matrix is given by

$$\mathbf{S}_1 = \mathbb{E}[\mathbf{z}\mathbf{z}^H | \mathcal{H}_1] = \begin{bmatrix} \mathbf{S}_s^{(1)} & \mathbf{S}_{sr} \\ \mathbf{S}_{sr}^H & \mathbf{S}_r \end{bmatrix}$$

where $\mathbf{S}_s^{(1)} = \mathbb{E}[\mathbf{z}_s \mathbf{z}_s^H | \mathcal{H}_1]$, $\mathbf{S}_{sr} = \mathbb{E}[\mathbf{z}_s \mathbf{z}_r^H | \mathcal{H}_1]$, and \mathbf{S}_r as before. Finally, we can reformulate the hypothesis test in (1) asymptotically in the frequency domain as

$$\begin{aligned} \mathcal{H}_0 : \quad & \mathbf{z} \sim \mathcal{CN}_{(J+K)LNP}(\mathbf{0}, \mathbf{S}_0), \\ \mathcal{H}_1 : \quad & \mathbf{z} \sim \mathcal{CN}_{(J+K)LNP}(\mathbf{0}, \mathbf{S}_1). \end{aligned}$$

Given M independent and identically distributed realizations of \mathbf{z} , $\mathbf{z}_0, \dots, \mathbf{z}_{M-1}$, and after some algebraic

reformulations, the generalized likelihood ratio (GLR) is given by

$$\begin{aligned}\mathcal{G}^{1/M} &= \det(\mathbf{D} - \mathbf{C}\mathbf{C}^H) \\ &= \det(\mathbf{D}) \det(\mathbf{I}_{KLN P} - \tilde{\mathbf{C}}^H \tilde{\mathbf{C}}),\end{aligned}\quad (2)$$

where

$$\begin{aligned}\mathbf{D} &= \left(\hat{\mathbf{S}}_s^{(0)}\right)^{-1/2} \hat{\mathbf{S}}_s^{(1)} \left(\hat{\mathbf{S}}_s^{(0)}\right)^{-1/2}, \\ \mathbf{C} &= \left(\hat{\mathbf{S}}_s^{(0)}\right)^{-1/2} \hat{\mathbf{S}}_{sr} \left(\hat{\mathbf{S}}_r\right)^{-1/2}, \\ \tilde{\mathbf{C}} &= \left(\hat{\mathbf{S}}_s^{(1)}\right)^{-1/2} \hat{\mathbf{S}}_{sr} \left(\hat{\mathbf{S}}_r\right)^{-1/2},\end{aligned}$$

and maximum likelihood (ML) estimates given by¹

$$\begin{aligned}\hat{\mathbf{S}}_s^{(0)} &= \text{diag}_L(\mathbf{Q}_s), \\ \hat{\mathbf{S}}_s^{(1)} &= \text{block}_{J,J} \text{diag}_{LP}(\mathbf{Q}_s), \\ \hat{\mathbf{S}}_{sr} &= \text{block}_{J,K} \text{diag}_{LP}(\mathbf{Q}_s), \\ \hat{\mathbf{S}}_r &= \text{block}_{K,K} \text{diag}_{LP}(\mathbf{Q}_s).\end{aligned}$$

In these expressions, the sample covariance matrix is

$$\mathbf{Q} = \frac{1}{M} \sum_{m=0}^{M-1} \mathbf{z}_m \mathbf{z}_m^H = \begin{bmatrix} \mathbf{Q}_s & \mathbf{Q}_{sr} \\ \mathbf{Q}_{rs} & \mathbf{Q}_r \end{bmatrix}.$$

Let us provide a brief interpretation of the test statistic (2): the first factor accounts for all combinations of the cyclic cross spectral correlations at multiple surveillance arrays, i.e., it is a generalization of the multivariate cyclostationarity detector [24] to multiple arrays. The second factor accounts for the additional information available through cross spectral correlations across all combinations of the signals at surveillance and reference arrays in the presence of a target. Then, this GLR shows how to fuse the information provided by the additional channels. Asymptotically, the detector has a constant false alarm rate (CFAR) with respect to the noise PSD at the SC and the signal-plus-noise PSD at the RC.

4. ASYMPTOTIC DISTRIBUTION UNDER THE NULL HYPOTHESIS

The GLR can be expressed as a ratio of determinants of the ML estimates of the covariance matrices $\hat{\mathbf{S}}_0$ and $\hat{\mathbf{S}}_1$. Since a properly selected permutation of $\hat{\mathbf{S}}_0$ and $\hat{\mathbf{S}}_1$ makes them block-diagonal, and generalizing [25], it can be shown that the distribution of the GLR statistic under the null hypothesis is given by a product of independent Beta random variables, that is

$$\mathcal{G}^{1/M} \stackrel{D}{=} \prod_{l=1}^N \left\{ \prod_{k=1}^{JP} \prod_{m=1}^L U_{k,m} \right\} \left\{ \prod_{n=1}^{KLP} V_n \right\}, \quad (3)$$

¹The operator $\text{block}_{L,M} \text{diag}_N(\mathbf{A})$ obtains an $L \times M$ block matrix from the matrix \mathbf{A} , where each block is a square block-diagonal matrix with block size N obtained from the respective block in \mathbf{A} , where \mathbf{A} is of suitable dimension.

where all U, V are independent Beta distributed random variables:

$$\begin{aligned}U_{k,m} &\sim \text{Beta}\{M - ((k-1)L + m - 1), (k-1)L\}, \\ V_n &\sim \text{Beta}\{M - (JLP + n - 1), JLP\}.\end{aligned}$$

Since (3) only depends on the known parameters J, K, L, P, M , and N , it allows us to generate offline the empirical distribution functions. These can be used to select the desired threshold for a given probability of false alarm.

5. NUMERICAL RESULTS

This section evaluates the performance of the proposed GLRT by means of Monte Carlo simulations. According to the model in (1), we generate the CS signal $\mathbf{s}[n]$ as a QPSK-signal with rectangular pulse shaping. The number of samples per symbol is equal to the cycle period P . Furthermore, the frequency-selective channels $\mathbf{H}_{s,j}[n]$ and $\mathbf{H}_{r,k}[n]$ are both Rayleigh-fading channels with a delay spread of 10 times the symbol duration and an exponential power delay profile. For all J, K , we generate $\mathbf{H}_{s,j}[n]$ and $\mathbf{H}_{r,k}[n]$, and $\mathbf{v}_{s,j}[n]$ and $\mathbf{v}_{r,k}[n]$ independently. Also note that new realizations of all parameters are drawn in each Monte Carlo simulation.

The SNR is defined as

$$\text{SNR}_\clubsuit = 10 \log_{10} \left(\frac{\text{tr}(\hat{\mathbf{R}}_\clubsuit)}{\text{tr}(\hat{\mathbf{V}}_\clubsuit)} \right),$$

where $\clubsuit \in \{s, r\}$ and

$$\begin{aligned}\hat{\mathbf{R}}_\clubsuit &= \frac{1}{MNP} \sum_{n=0}^{MNP-1} \mathbf{h}_\clubsuit[n] \mathbf{h}_\clubsuit^H[n], \\ \hat{\mathbf{V}}_\clubsuit &= \frac{1}{MNP} \sum_{n=0}^{MNP-1} \mathbf{v}_\clubsuit[n] \mathbf{v}_\clubsuit^H[n],\end{aligned}$$

with $\mathbf{h}_\clubsuit[n] = \left[(\mathbf{H}_{\clubsuit,1}[n] * \mathbf{s}[n])^T \ (\mathbf{H}_{\clubsuit,2}[n] * \mathbf{s}[n])^T \ \cdots \right]^T$, and similarly, $\mathbf{v}_s[n] = [\mathbf{v}_{s,1}^T[n] \ \cdots \ \mathbf{v}_{s,J}^T[n]]$ and $\mathbf{v}_r[n] = [\mathbf{v}_{r,1}^T[n] \ \cdots \ \mathbf{v}_{r,K}^T[n]]$. Hence, the SNR is as an average across all surveillance and reference arrays, respectively.

In order to evaluate the performance of the proposed GLR, we generalize the correlated subspace detector, denoted as \mathcal{K} and proposed in [9], to the case of multiple surveillance and reference arrays by treating them as two large arrays of dimensions JL and KL , respectively. The second competitor is the multiarray extension of the popular cross-correlation detector [6], denoted as \mathcal{C} . It should be noted that the cross-correlation detector does not require any prior knowledge, whereas the correlated subspace detector needs to know the number of antennas L_I at the IO, and our proposed technique also needs to know the cycle period P . Generally, both P and L_I could be estimated or

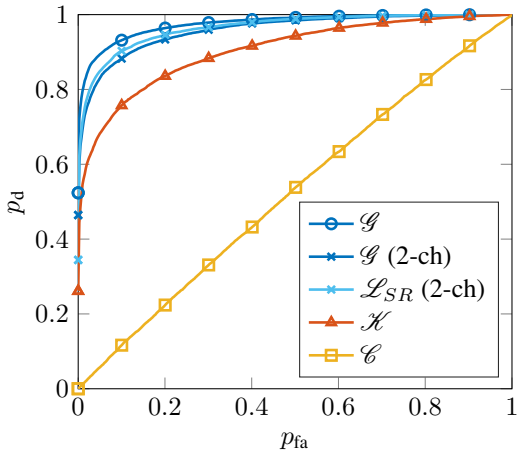


Fig. 1: ROC curves in a scenario with $P = 2$, $N = 16$, $M = 64$, $L = L_I = 2$, a rectangular pulse, $\text{SNR}_s = \text{SNR}_r = -20$ dBs, and an equal number of surveillance and reference arrays $J = K = 5$.

they may be known from the standards used by the IO. Additionally, we also compare the proposed detector to our previously derived two-channel detectors from [12] by treating the J surveillance arrays with L antennas each as one large array with JL antennas and similarly, the reference arrays are treated as another large array with KL antennas. The two-channel GLRT is denoted as \mathcal{G} (2-ch) and the two-channel LMPIT-inspired test is denoted as \mathcal{L}_{SR} (2-ch).

In Figure 1 we investigate the receiver operating characteristic (ROC) curve for $\text{SNR}_s = \text{SNR}_r = -20$ dBs in the case of an equal number of arrays at surveillance and reference arrays, i.e., $J = K = 5$. We can observe that the GLRT, denoted as \mathcal{G} , performs best. The two-channel detectors from [12] perform second best. They are followed by \mathcal{K} and the cross-correlation detector is almost the chance line. The reason for the poor performance of the cross-correlation detector is the low SNR regime, as it was similarly observed in [12]. Since the performance of this detector is particularly bad, we will neglect it in further figures as it does not provide further insight. The gap between the multichannel detectors and the two-channel detectors can be explained by the fact that the two-channel detectors inherently presumes a different noise structure than the one present in the data generation. Specifically, the two-channel detectors overfit the underlying noise model as they presume more degrees of freedom than those actually present.

Now, we choose all parameters as before and keep the total number of arrays constant but increase the number of surveillance arrays to $J = 8$ and decrease the number of reference arrays to $K = 2$. Figure 2 shows that the GLRT \mathcal{G} performs best followed by the two-channel detectors. Note that the order of the two-channel GLRT and the

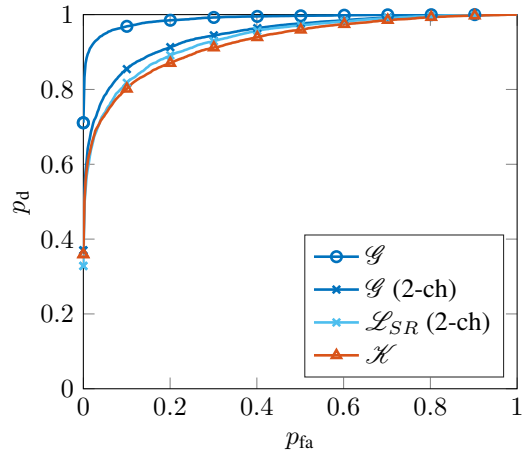


Fig. 2: ROC curves in a scenario with $P = 2$, $N = 16$, $M = 64$, $L = L_I = 2$, a rectangular pulse, $\text{SNR}_s = \text{SNR}_r = -20$ dBs, $J = 8$ surveillance, and $K = 2$ reference arrays.

two-channel LMPIT-inspired test has changed. This can be explained by the fact that the GLRT combines spectral correlations within the surveillance array with the cross-correlations between SC and RC. Since for this scenario we have more surveillance arrays than reference arrays, it is more beneficial to include the inter-SC correlations rather than only accounting for the cross-spectral correlations only as it is done by the two-channel LMPIT-inspired test [12]. The correlated subspace detector performs similarly to the two-channel LMPIT-inspired test.

6. CONCLUSION

We have derived the GLRT for the detection of cyclostationary signals given multiple surveillance and reference arrays. The derived detector exploits the cross spectral correlations across all surveillance channels induced by the cyclostationary properties of the target echo and the cross (spectral) correlations across the surveillance and reference arrays to detect the presence of a cyclostationary signal at the surveillance channels. Numerical simulations have shown that it outperforms competing techniques.

7. REFERENCES

- [1] P.E. Howland, D. Maksimiuk, and G. Reitsma, "FM radio based bistatic radar," *IEE Proc. Radar, Sonar, Navig.*, vol. 152, no. 3, pp. 107–115, June 2005.
- [2] K.S. Kulpa and Z. Czekala, "Masking effect and its removal in PCL radar," *IEE Proc. Radar, Sonar, Navig.*, vol. 152, no. 3, pp. 174–178, June 2005.
- [3] F. Colone, D.W. O'Hagan, P. Lombardo, and C.J. Baker, "A Multistage Processing Algorithm for Dis-

- turbance Removal and Target Detection in Passive Bistatic Radar,” *IEEE Trans. on Aerospace, Electr. Syst.*, vol. 45, no. 2, pp. 698–722, Apr. 2009.
- [4] F. Colone, R. Cardinali, P. Lombardo, O. Crognale, A. Cosmi, A. Lauri, and T. Bucciarelli, “Space-time constant modulus algorithm for multipath removal on the reference signal exploited by passive bistatic radar,” *IET Radar, Sonar, Navig.*, vol. 3, no. 3, pp. 253–264, 2009.
- [5] G.E. Smith, K. Chetty, C.J. Baker, and K. Woodbridge, “Extended time processing for passive bistatic radar,” *IET Radar, Sonar, Navig.*, vol. 7, no. 9, pp. 1012–1018, Dec. 2013.
- [6] J. Liu, H. Li, and B. Himed, “On the performance of the cross-correlation detector for passive radar applications,” *Signal Process.*, vol. 113, pp. 32–37, 2015.
- [7] I. Santamaría, L. L. Scharf, D. Cochran, and J. Vía, “Passive detection of rank-one signals with a multi-antenna reference channel,” in *Proc. European Signal Proc. Conf.*, Budapest, Hungary, 2016, pp. 140–144.
- [8] H. Wang, Y. Wang, L. L. Scharf, and I. Santamaría, “Canonical correlations for target detection in a passive radar network,” in *Proc. Asilomar Conf. Signals, Syst., Comput.*, Pacific Grove, CA, USA, 2016, pp. 1159 – 1163.
- [9] I. Santamaría, L. L. Scharf, J. Vía, H. Wang, and Y. Wang, “Passive detection of correlated subspace signals in two MIMO channels,” *IEEE Trans. on Signal Process.*, vol. 65, no. 20, pp. 5266–5280, Oct. 2017.
- [10] S. Horstmann, D. Ramírez, and P. J. Schreier, “Two-channel passive detection exploiting cyclostationarity,” in *Proc. European Signal Proc. Conf.*, A Coruña, Spain, 2019.
- [11] S. Horstmann, D. Ramírez, P. J. Schreier, and A. Pries, “Two-channel passive detection of cyclostationary signals in noise with spatio-temporal structure,” in *Proc. Asilomar Conf. Signals, Syst., Comput.*, Pacific Grove, CA, USA, Nov. 2019, pp. 1333–1337, IEEE.
- [12] S. Horstmann, D. Ramírez, and P. J. Schreier, “Two-Channel Passive Detection of Cyclostationary Signals,” *IEEE Trans. Signal Process.*, vol. 68, pp. 2340–2355, 2020.
- [13] S. D. Howard and S. Sirianunpiboon, “Passive radar detection using multiple transmitters,” in *Proc. Asilomar Conf. Signals, Syst., Comput.*, Pacific Grove, CA, USA, Nov. 2013, pp. 945–948.
- [14] D. E. Hack, L. K. Patton, and B. Himed, “Detection in passive MIMO radar networks,” *IEEE Trans. Signal Process.*, vol. 62, no. 11, pp. 780–785, June 2014.
- [15] S. D. Howard, S. Sirianunpiboon, and D. Cochran, “An exact Bayesian detector for multistatic passive radar,” in *Proc. Asilomar Conf. Signals, Syst., Comput.*, Pacific Grove, CA, USA, Nov. 2016, pp. 1077–1080.
- [16] K. S Bialkowski, I. V. L. Clarkson, and S. D Howard, “Generalized canonical correlation for passive multistatic radar detection,” in *Proc. IEEE Stat. Sig. Proc. Work.*, Nice, France, 2011, pp. 417–420.
- [17] D. Cochran, H. Gish, and D. Sinno, “A geometric approach to multiple-channel signal detection,” *IEEE Trans. Signal Process.*, vol. 43, no. 9, pp. 2049–2057, Sept. 1995.
- [18] Y. Liu, G. Liao, H. Li, S. Zhu, Y. Li, and Y. Yin, “Passive MIMO radar detection with unknown colored Gaussian noise,” *Remote Sensing*, vol. 13, no. 14, 2021.
- [19] H.D. Griffiths and C.J. Baker, *An Introduction to Passive Radar*, Artech House, 2017.
- [20] R. Tao, H.Z. Wu, and T. Shan, “Direct-path suppression by spatial filtering in digital television terrestrial broadcasting-based passive radar,” *IET Radar, Sonar, Navig.*, vol. 4, no. 6, pp. 791–805, Sept. 2010.
- [21] A. Zaimbashi, M. Derakhtian, and A. Sheikhi, “GLRT-based CFAR detection in passive bistatic radar,” *IEEE Trans. on Aerospace, Electr. Syst.*, vol. 49, no. 1, pp. 134–159, 2013.
- [22] D. Ramírez, I. Santamaría, L. L. Scharf, and S. Van Vaerenbergh, “Multi-channel factor analysis with common and unique factors,” *IEEE Trans. Signal Process.*, vol. 68, pp. 113–126, 2020.
- [23] S. Searle and S. D. Howard, “Clutter cancellation in passive radar as a dual basis projection,” in *Proc. Asilomar Conf. Signals, Syst., Comput.*, Pacific Grove, CA, USA, Nov. 2019.
- [24] D. Ramírez, P. J. Schreier, J. Vía, I. Santamaría, and L. L. Scharf, “Detection of multivariate cyclostationarity,” *IEEE Trans. Signal Process.*, vol. 63, no. 20, pp. 5395–5408, Oct. 2015.
- [25] N. H. Klausner, M. R. Azimi-Sadjadi, and L. L. Scharf, “Detection of spatially correlated time series from a network of sensor arrays,” *IEEE Trans. Signal Process.*, vol. 62, no. 6, pp. 1396–1407, Mar. 2014.